IAC-24-D3.3.14

Multi-Objective Design Optimisation and Analysis of a Crewed Earth-Mars Transportation System using Nuclear Thermal Propulsion

Ben Parsonage* **and Christie Maddock**

Aerospace Centre of Excellence, University of Strathclyde, Glasgow G1 1XJ, United Kingdom
* *Corresponding author: ben.parsonage@strath.ac.uk*

Abstract

Establishing a human scientific settlement on Mars will require significant collaborative development across several important areas. In particular, an efficient and effective interplanetary transportation paradigm to support both initial and sustained future development of surface-based activity. The technological challenges of such an architecture will necessitate a synergistic amalgamation of novel technologies within fields such as propulsion, long-duration habitation, radiation mitigation and mission design, including the use of in-orbit structural assembly and re-fuelling.

The aim of this paper is to identify systems-level design drivers for a crewed interplanetary transportation solution to support future scientific settlement on Mars. Numerical models were developed to broadly represent current and near-future propulsion systems (with a particular focus on Nuclear Thermal Propulsion), habitation modules, nuclear/cosmic radiation exposure, power systems and vehicle structure. Models were then integrated into a multi-objective problem formulation examining both the static system/mission design parameters (e.g. planetary conjunction angles, dry/wet masses and engine system sizing) and the optimal trade-offs between outbound/inbound transfer trajectories for a variable surface stay duration on/around Mars. The problem was solved using a novel adaptive-mesh evolutionary solver for multi-objective optimal control problems.

Results suggest that the relative duration of mission segments (outbound, stay, inbound) conform to distinct groups of solutions within objective space. This represents a quantifiable set of transfer opportunities/mission architectures differentiated by total propellant requirements and the desired duration of surface activities at Mars. Furthermore, considering Nuclear Thermal Propulsion (NTP) technology, a tendency to reduce the size of the propulsion system towards the lower end of the performance spectrum is observed. This implies that current/future development should focus on improving system reliability, including investigations into extended operational cycles and restartability, rather than base performance statistics.

Keywords: Multi-Objective Optimisation, Nuclear Thermal Propulsion, Interplanetary Transportation

1 Introduction

An established limiting factor for crewed interplanetary exploration missions to Mars is the health risks posed by increased exposure to solar and cosmic radiation [1]. Given the directly proportional relationship between total dose and radiation flux/time of exposure, logical mitigation strategies include either reducing the radiation dosage via some form of protective shielding, or decreasing the interplanetary transfer time. Research into active/passive shielding is ongoing, but it is currently accepted that with the significant volume of shielding required for a Hohmann-type transfer to Mars, the costs to deliver this additional payload to LEO would be largely prohibitive to the overall mission. As such, it is prudent to examine the propulsion options available to instead reduce the time of flight. While conventional LO2/LH2 or LO2/LCH4 chemical propulsion systems may still remain the most practical option for Earth orbit and Lunar missions, their characteristic high thrust/low specific impulse results in largely infeasible mass fractions when applied to interplanetary trajectories. Given the resultant need for higher power density and specific impulse I_{sp}, a viable alternative is the use of nuclear propulsion.

As early as the 1940s, nuclear derived technology was recognised as a fundamental enabler for future space travel. Landmark studies, such as [2] concerning Nuclear Thermal Rocketry (NTR) and Nuclear Electric Propulsion (NEP) for interplanetary trajectories, helped prompt initial investigations into the practicalities of nuclear propulsion systems. Subsequent work included the Soviet NTR engine development program [3], the Atomic Energy Commission 'Project Rover' [4] and the NASA Nuclear Engine for Rocket Vehicle Application (NERVA) program [5], the latter incorporating a promising series of successful terrestrial test firings, prompting inclusion into several proposals for crewed missions to Mars [6, 7]. Since then, advances in materials, magnetic fields and plasma dynamics have supported the development of numerous appealing concepts [8]. Currently, many space agencies and governments (e.g. NASA and DARPA, ESA, UKSA, Roscomos, China, and India) have programmes examining nuclear propulsion for space

Mission	Engine	Cluster	Power (MW)	Thrust (kN)	$\dot{m}$ (kg/s)	Mass (kg)
DRA 5.0	Pewee-1	3	1521	333.6	37.8	9900
MEC	NRE 68 kN	4	1360	272	28.4	11560
Aerojet	AR-NTP	3	1627.2	334.8	38.1	11380

Table 2: Clustered NTP systems in existing crewed Mars mission concepts, sourced from [16], [22] and [24].

	Crew = 6			Crew = 4	
Component	Mass [kg]	Vol. [m^3]	% red.	Mass [kg]	Vol. [m^3]
Power system	5840	–	22.5	4526	–
Avionics	290	0.1	0	290	0.1
ECLSS	3950	19.1	15	3357.5	16.235
TMS	1260	5.3	15	1071	4.505
Crew accommodations	4210	29.7	22.5	3262.75	23.0175
EVA systems	870	2.9	30	609	2.03
Structure	2020	–	22.5	1565.5	
(inc. 30% margin)	4920			3934.875	
Spares	4180	1.4	15	3553	1.19
Crew	6×80	–	–	4×80	–
Radiation shelter	6×739.36			4×739.36	
Total (no consumables)	32536.16			25447.06	

Table 3: Mass breakdown, adapted from [16, 26] with radiation 'storm' shelter estimate from [27].

711 kW) orbits for reference.

$$G_{SC} = \epsilon \sigma T^4 \frac{4\pi R_{sun}^2}{4\pi R^2} \tag{1}$$

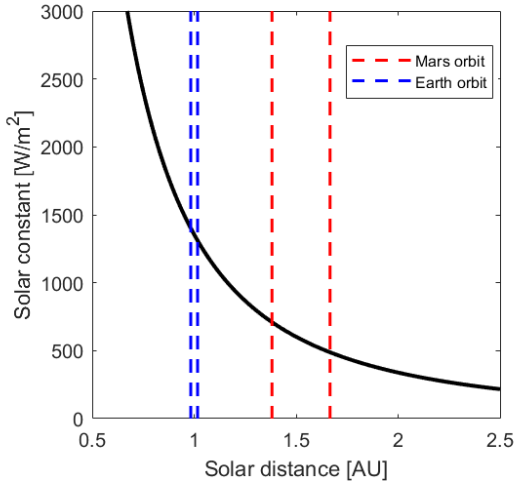

Figure 1: Solar constant at Earth and Mars.

Assuming PVA specifications in line with the NASA DRA (i.e., specific mass of 2 kg/m^2, power generation 0.12 kW/m^2 and 25% efficiency), the minimum required area of PVA can be taken as 500m^2, with an equivalent mass of 1000kg. However, the lateral diameter (and thus available area) of the panels will be constrained by the radiation shield shadow, given the detrimental effects of radiation on sensitive electronics.

2.1.4 Thermal Management

NTP systems utilise open-cycle cooling, where waste heat is ejected both by thermal radiation and exhaust convection. Unlike NEP systems then, NTP systems do not typically require a significantly large thermal management system, with the highest system demands likely present during engine cooldown. For this reason, thermal radiators (and any associated mass penalty) are not considered in detail within this study.

2.1.5 Radiation

Concerning modern understanding of the undesirable biological effects associated with long-duration space habi-

tation, human health considerations potentially represent the most demanding performance constraints for future interplanetary expeditions. Translated mission/vehicle design requirements relevant to the mitigation of acute and chronic risks associated to radiation exposure may be defined as follows:

- **Total accumulated dose for a single crew member must not exceed 500mSv.** This corresponds to a one-way transfer time of 90 days, a Mars surface stay of 525 days, solar minimum conditions and spacecraft shielding equivalent to 5g/cm^2 Al [29].
- **The Crew Transport Vehicle (CTV) must include a dedicated means of protection against intense SPE radiation.** Such shelter, either internal or external, must provide radiation shielding equivalent to 20-35g/cm^2 Al [30].
- **Additional radiation due to nuclear propulsion must be minimised.** This includes considerations of component layout (for habitat occlusion), spacecraft length, reactor size, impulse duration/frequency and multi-layer external radiation shield sizing.

To incorporate these requirements into the following analyses, approximate relationships for expected radiation dose during transit and surface operations at Mars are defined (see Figure 2) [29]. The latter is relevant given the availability of interplanetary transfer windows for a desired flight duration. As such, should the surface stay be of a necessarily long duration in comparison to the transit, additional environmental radiation dosage should be accounted for.

During transit, Galactic Cosmic Radiation (GCR) shielding equivalent to 5g/cm^2 Al is assumed for the crew habitation module [20]. Solar minimum conditions are considered for two primary reasons. First, missions during solar minimum are less likely to be affected by extreme Solar Particle Events (SPEs), despite the larger GCR dosage. Furthermore, there is currently no reliable method of accurately predicting extreme SPEs, though they are know to occur at least once annually during 9 out of the 11 years in a solar cycle. Secondly, as this study does not assume any specific launch date, taking solar minimum conditions therefore gives a conservative estimate of radiation dosage. In the case of SPEs, the crew may take refuge in a small shelter housed either within the crew habitation module or components of the external structure. For example, a radiation shelter housed between the hydrogen propellant tanks, as in [15], or a docked orbital return vehicle (e.g. an Orion capsule), as in [16]. For this study, internal crew quarters are assumed to represent option (3) as presented by [27], providing heavy radiation shielding equivalent to at least 20 g/cm^2 Al at a mass penalty of 739.36 kg/crew. Shelters may be utilised both to protect from SPEs and during nominal crew sleep cycles.

Based on the data presented in [29], the rates of expected radiation dosage relative to transit time and surface stay time (assuming solar minimum conditions and radiation shielding equivalent to either 5 or 20 g/cm^2) are:

$$r_{transit(5)} = 1.7309 \text{ mSv/day} \tag{2}$$

$$r_{transit(20)} = 1.4017 \text{ mSv/day} \tag{3}$$

$$r_{stay} = 0.32423 \text{ mSv/day} \tag{4}$$

Of note, the reported dosage rate for the surface portion of the mission may be significantly reduced by constructing a heavily shielded surface habitat, e.g., by exploiting Martian regolith, as in [14, 29].

To dimension the external radiation shield, the methodology presented in [31] is adopted. Using material data originally reported in [32], the work [31] analyses different material configurations using the Monte-Carlo N-Particle Transport (MCNP) method to define simplified expressions for neutron fluence and gamma dose, where maximum allowable values were assumed 4.455e9 n/cm^2 and 15 rad, respectively. Assuming the NTP system is powered on only to perform the impulsive manoeuvres, the additional radiation dosage to the crew may be estimated.

The mitigation of additional radiation exposure due to the onboard nuclear reactor includes implications for the design/structural layout of the vehicle. Firstly, dosage decreases proportional to the squared distance relative to the radiation source, thus the length of the vehicle truss L_{truss} is to be maximised within loading/buckling constraints (largely determined by the propulsion system). Furthermore, the length of truss, coupled with the diameter of the radiation shield, then determines the maximum lateral spread of components such as radiators or PVAs, given the requirement for all mission critical components to lie within the radiation shadow cone.

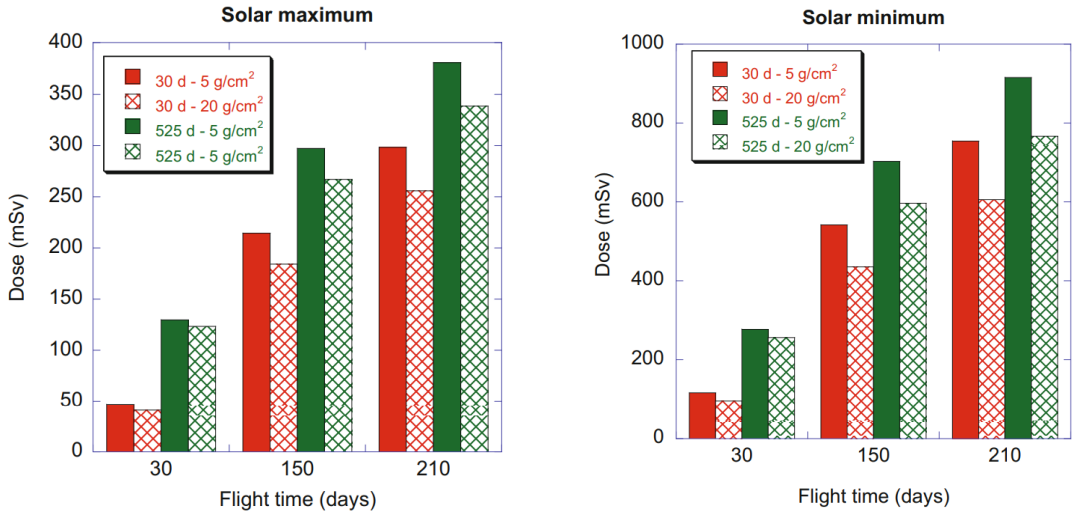

(a) (b)

Figure 2: Estimated total equivalent doses for a Mars mission. Green bars are relative to a long stay on the Mars base (over 1 year), red bars for a Mars sortie (30 days on the planet). Solid bars are calculations for a spacecraft with a minimum shield (5 g/cm^2 Al); dashed bars for a thick shield in the spacecraft (20 g/cm^2 Al). All doses are calculated assuming the dose rate of the 1970 solar maximum [29].

2.1.6 Spacecraft structure

To account for the mass of components such as propellant tanks, external subsystems (e.g., communications arrays) and external structure (e.g., truss), the overall structural mass is assumed 10% of the initial spacecraft mass in LEO.

2.2 Flight dynamics

The vehicle dynamics are defined via the following expressions for the rates of change of state vector $\mathbf{x} = [r, \theta, v_r, v_\theta, m_{prop}, m_{cons}]$ in an inertial reference frame, where r is the radial distance from the centre of the current Sphere of Influence (SOI), θ is the angular position, v_r is the radial velocity, v_θ is the angular velocity, m_{prop} is the mass of propellant and m_{cons} is the mass of consumables.

$$\dot{r} = v_r \tag{5}$$

$$\dot{\theta} = \frac{v_\theta}{r} \tag{6}$$

$$\dot{v}_r = \frac{v_\theta^2}{r} - \frac{\mu}{r^2} + \frac{\tau T_{max}}{m} \sin \alpha_{eng} \tag{7}$$

$$\dot{v}_\theta = -\frac{v_r v_\theta}{r} + \frac{\tau T_{max}}{m} \cos \alpha_{eng} \tag{8}$$

$$\dot{m}_{prop} = -\tau \dot{m}_{prop} \tag{9}$$

The scalar variable $\tau = [0,\ 1]$ is the throttle controlling the fraction of thrust applied, α_{eng} is the angle of the thrust vector and T_{max} is the maximum available engine thrust. The SOI for both Earth and Mars is given by,

$$SOI = a_{\text{E/M}} \left(\frac{m_{\text{E/M}}}{m_{sun}} \right)^{2/5} \tag{10}$$

where a is the semi-major axis and m is the planetary mass. A further assumption is that of perfectly circular orbits of Earth and Mars. This is to disentangle the initial mission analysis from dependence on considering specific launch dates/windows, instead allowing a more general approach that may be applicable across many future scenarios. The reference frames are centred on the primary gravitational body (either Earth, the Sun, or Mars) depending on the mission phase.

3 Approach

The complete mission profile is divided into three distinct segments: the outbound Earth to Mars (EM) transfer, the stay time at Mars, and the inbound Mars to Earth (ME) transfer. Each interplanetary segment is composed of three phases: low-altitude planetary departure, interplanetary transfer and planetary capture to low altitude orbit.

The relationship between the primary mission segments is examined with respect to spacecraft design parameters

by formulating a sequence of multi-objective optimal control problems (MOCPs). Of particular interest are the relative durations between each segment and the phasing between the outbound and inbound transfers.

Continuous control profiles for engine thrust were included to determine the optimal switching structure for each segment. More specifically, the engine throttle is defined as a continuous parameter evaluated at the control nodes.

The MOCP objectives were taken as the minimisation of total interplanetary transfer time (i.e., not including the stay time at Mars), and the gross vehicle mass (including any in-orbit refuelling whilst in LMO).

$$\min_{\mathbf{u}\in\mathbf{U},\mathbf{d}\in\mathbf{D}} \sum_{i=1}^{N} (t_{f,i} - t_{0,i}) \tag{11a}$$

$$\min_{\mathbf{u}\in\mathbf{U},\mathbf{d}\in\mathbf{D}} m(t_0) \tag{11b}$$

where N is the number of flight trajectory phases defined, t_0 and t_f are the initial and final times respectively, and

$$\mathbf{u} = \begin{bmatrix} \boldsymbol{\alpha}_i & \boldsymbol{\tau}_i & (\Delta t)_i \end{bmatrix} \tag{12}$$

is the trajectory control vector where $(\Delta t)_i = t_{f,i} - t_{0,i}$ is the time of flight for the i^{th} phase, $\boldsymbol{\alpha}$ is the set of thrust direction angles and $\boldsymbol{\tau}$ is the set of throttle values at every control node in the the i^{th} phase. The optimisation vector of static design parameters is given by,

$$\mathbf{d} = \begin{bmatrix} \phi_p(t_0) & P_{eng} & m_{str} \end{bmatrix} \tag{13}$$

where ϕ_p is the angle between Earth and Mars at the initial time, P_{eng} is the reactor power, m_{str} is the structural mass of the spacecraft. The gross mass $m_0 = m(t_0)$ is a sum of the calculated masses for the structure, engine system, propellant and tanks, crew, habitat and consumables.

The following additional assumptions were included:

- Prior to each transfer, the spacecraft is assumed positioned in a circular low-altitude planetary parking orbit (LEO, or LMO).
- A Sphere of Influence (SOI) trajectory approach is adopted, where the spacecraft is assumed affected by only the dominant gravitational force of the current phase.
- No advanced mid-flight events, e.g., mass jettisoning, refuelling, aero-braking or gravity assist flybys are considered, though the optimiser may include deep space manoeuvres whilst in interplanetary space.

3.1 Optimisation algorithm

This work employs the mesh-adaptive Multi-Agent Collaborative Search (MACS) algorithm as described in the works [33, 34]. This algorithm solves multi-objective optimal control problems using a direct approach, with individualistic grid adaptation facilitated by a local error analysis at element boundaries. Multiple objectives are considered using a dominance-based memetic framework applying both local and global search methods to a collaborative population of unique solutions. Together, this avoids the need for *a priori* specification of the quantity and temporal location of element boundaries, and the set of scalarisation weights defining the multi-objective descent directions. Solution fidelity can thus increase concurrently with the exploration of the design space, which leads to increased numerical efficiency, particularly for discontinuous or highly non-linear problems, whilst propagating and maintaining population diversity.

In the following, system state and control profiles are represented using element-specific 9^{th} order Bernstein polynomials. A population of 10 solution vectors was initially discretised upon a uniform grid. Solution-specific grid adaptation was performed every 20 iterations, where the relative local error tolerance was set to $\epsilon_{tol} \leq 10^{-6}$. Inner-level optimisation was completed using the MATLAB $\mathrm{fmincon}$ solver with a SQP algorithm where function, constraint violation and step tolerances are set to 1e-6, 1e-12 and 1e-9 respectively. Each process was terminated upon reaching a maximum number of iterations, $n_{iter,max} = 200$.

4 Results

Results are presented for a full mission, including an outbound transfer, a period of time spent in the vicinity of Mars, and a return transfer. First, the initial outbound transfer was analysed separately, with results used to construct a set of interpolating surrogates representing the corresponding design parameters. These relationships were then used to analyse the complete mission with a reduced NLP size. Both analyses were formulated to minimise the time spent in transit (thus minimising the radiation risk to the crew), whilst simultaneously minimising the total propellant requirement (and thus cost).

4.1 Earth-Mars Transfer

The outbound EM transfer consists of three phases. The first assumes the spacecraft is initially positioned in LEO and bound to the Earth's gravitational field within the boundaries of the Earth's SOI. The second phase assumes a heliocentric orbit, influenced only by the Sun's gravity. Finally, the third phase assumes the spacecraft is influenced only by Mars, again within the boundaries of the corresponding SOI, with a fixed final state in LMO.

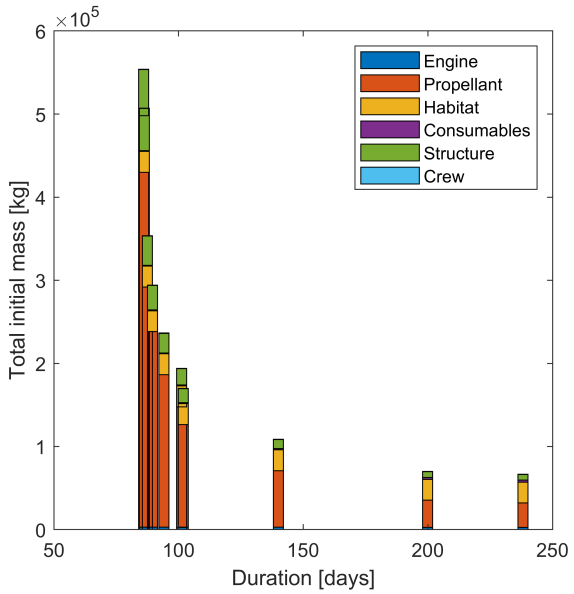

Figure 3: Outbound EM transfer: Total initial mass breakdown against transfer duration.

The vehicle is controlled by continuously varying both the magnitude and direction of the engine thrust, the former given the documented throttling capabilities of NTP systems [5]. The maximum thrust and mass flow rate of the engine, as well as it's overall mass, are dependant on a static optimisable parameter representing the thermal power of the reactor (see Section 2.1.1).

Figure 3 shows the mass breakdown of Pareto-optimal solutions obtained for the initial outbound mission segment. In line with traditional analyses of NTP systems (and conforming to the expected norms established by CP systems), the primary driver is seen to be the propellant mass, directly related to the ΔV requirement for a particular transfer trajectory. This can be seen most clearly via comparison between the minimum-mass and minimum-time solutions, shown respectively in Figures 4 and 5. The minimum-mass solution here corresponds to the low-energy *conjunction* class transfer common in Mars mission analyses.

#	t_{EM} [days]	m_{EM} [kg]	θ_{init} [deg]	P_{eng} [MW]	T_{eng} [kN]
1	86.0	5.54e5	17.2	406.5	83.9
2	86.3	5.07e5	17.2	381.2	78.1
3	87.5	3.54e5	17.8	377.8	77.3
4	89.6	2.94e5	17.8	381.1	78.0
5	94.1	2.36e5	18.3	391.5	80.5
6	101.2	1.94e5	18.9	308.8	61.3
7	101.9	1.70e5	20.1	389.0	79.9
8	140.1	1.09e5	29.8	372.4	76.0
9	199.9	0.70e5	32.7	321.4	64.2
10	238.1	0.67e5	38.4	319.7	63.8

Table 4: Outbound EM transfer: Design parameters.

Table 4 summarises the design parameters of each Pareto-optimal solution. The optimiser is seen to favour NTP engines at the lower end of the performance spectrum represented by the engine sizing model (Section 2.1.1), generally preferring longer, sustained manoeuvres rather than short and intensive (particularly as transfer duration decreases). Importantly, the system is seen to be capable of a EM transfer duration of less than 90 days, corresponding to the original mission requirements.

4.2 Earth-Mars-Earth Transfer

The inbound transfer follows a period of time spent in the vicinity of Mars. To relate the planetary phasing at the commencement of the return leg to the overall mission timeframe, the initial outbound transfer duration and the Mars stay time are both included as optimisable static variables. To include the penalty associated to the outbound transfer duration and propellant expenditure, the Pareto-set presented in Section 4.1 are used to generate a set of continuous interpolating surrogate models representing relevant parameters of the EM transfer segment. These relationships, depicted in Figure 6, are made available to the optimiser such that the complete mission profile may be examined with continuity, but also with a significantly reduced NLP size. With regards to the depletable vehicle states, i.e. propellant and consumable masses, the availability of in-orbit manufacturing/refuelling whilst in LMO is assumed (and included in the calculation of total system mass).

Figure 7 shows the Pareto-set relating to the (a) outbound transfer and (b) inbound transfer, colour coded to

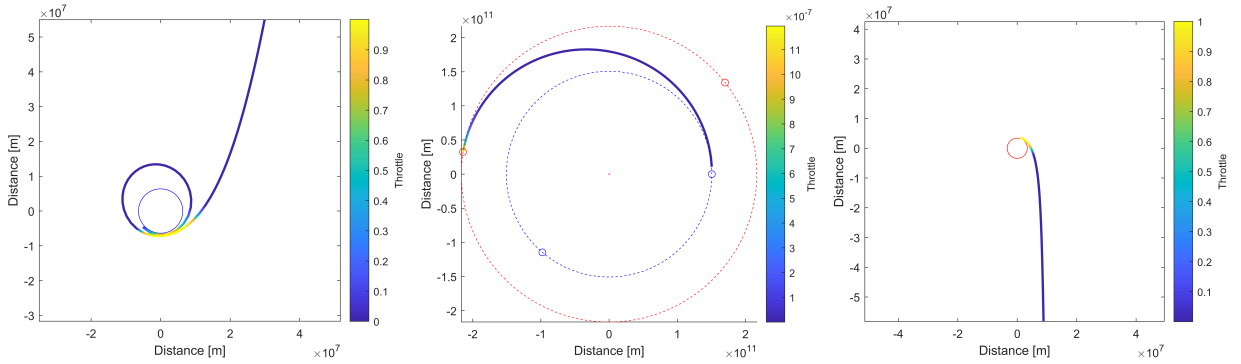

(a) (b) (c)

Figure 4: Outbound EM transfer: Minimum-mass solution.

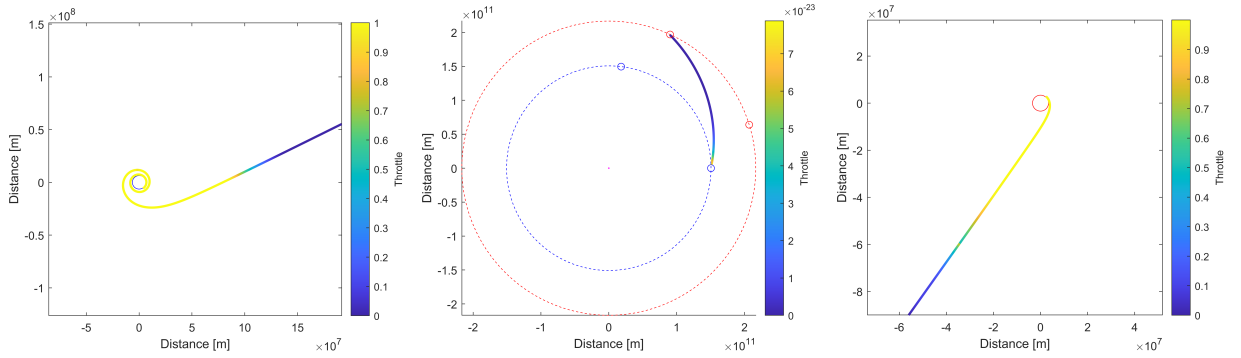

(a) (b) (c)

Figure 5: Outbound EM transfer: Minimum-time solution.

represent the total system mass. Table 5 lists the design parameters corresponding to each solution of the inbound MOCP. With regards to the inbound trajectories specifically, two distinct clusters may be seen. One contains the minimum-mass profiles. Each of these first performs a conjunction class outbound transfer. The stay time at Mars is then seen to be either very long (250-400 days) or very short ($\tilde{3}$0 days). The short stay solutions correspond to the two longest inbound transfers, thus it may be suggested that the switch back to short-stay from long-stay is triggered by the relative phasing between Earth and Mars. The minimum-mass solutions naturally exhibit the longest transfer durations, even passing outside the orbit of Mars during the inbound segment, thus may only be suitable for crewed expeditions provided an appropriate advancement in radiation shielding technology. The other contains the minimum-time profiles. These solutions all require the minimum allowable stay time at Mars (30 days), before immediately embarking on the return leg, itself corresponding to the traditional *opposition* class transfer. This class of transfer is usually identified as being unsuitable for crewed expeditions given the closer proximity to the Sun, thus inducing an increased dose of radiation to the crew. Furthermore, whilst the outbound transfer is capable of lying under the 90 day cutoff, the shortest return leg is seen to be almost double this value, despite the vastly increased propellant requirement.

The propulsion system design parameters for the complete outbound/inbound mission are seen to follow the same trend as when examining the outbound transfer on it's own. That is, a tendency to lie within the lower end of the performance spectrum summarised in Table 1. This itself suggests that future development of NTP technology should be more focused on improving system reliability, particularly with respect to extended operational cycles and restartability, rather than base performance statistics.

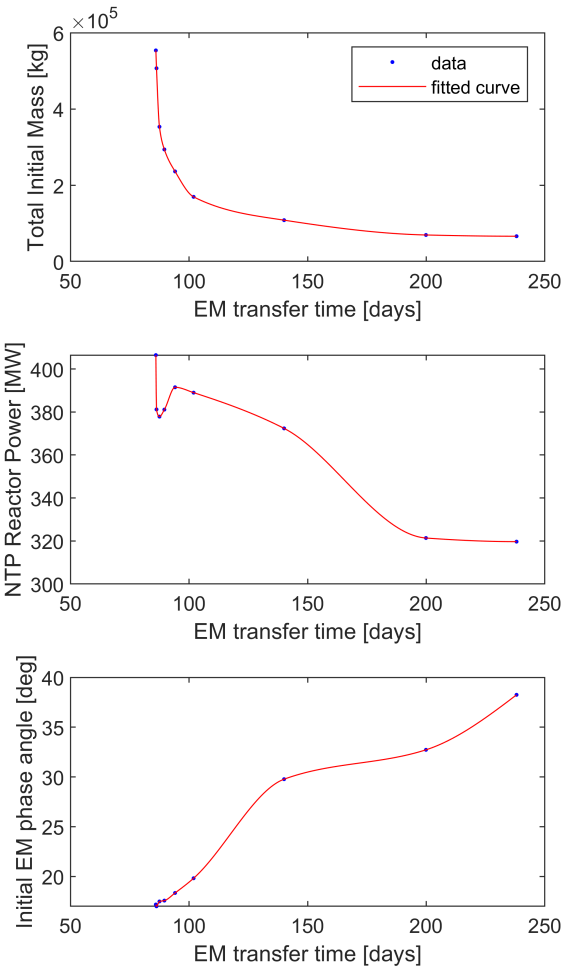

Figure 6: Outbound EM transfer parameter surrogates.

#	t_{EM} [days]	t_{stay} [days]	t_{ME} [days]	m_{EM} [kg]	m_{ME} [kg]	P_{eng} [MW]
1	236.0	30.0	646.7	0.67e5	1.84e5	319.7
2	236.2	30.1	614.6	0.67e5	2.06e5	319.7
3	198.3	250.1	472.2	0.70e5	2.08e5	321.6
4	187.4	356.9	376.4	0.74e5	2.26e5	326.6
5	179.5	399.6	341.7	0.77e5	2.38e5	333.3
6	112.9	30.0	215.5	1.42e5	4.18e5	384.9
7	106.8	30.0	203.5	1.56e5	4.84e5	387.2
8	101.8	30.0	190.5	1.70e5	5.59e5	389.0
9	101.3	30.0	172.2	1.72e5	7.01e5	389.2
10	98.9	30.0	173.4	1.89e5	7.26e5	390.2

Table 5: Complete EME mission parameters.

5 Conclusion

A set of continuous numerical models representing the major subsystems of a crewed interplanetary transport vehicle were developed. Vehicle and mission performance design trade-offs were examined within a multi-disciplinary design optimisation framework.

The presented problem focused on optimising the vehicle design and mission phasing. More specifically, the engine sizing, propellant mass, dry mass (including the required mass of consumables) and the outbound/inbound trajectories (including a period of time spent at Mars). The transfer trajectory from Earth to Mars was first evaluated separately. The results of this analysis were used to generate simple numerical relationships representative of the outbound transfer design parameters. These relationships were then used to examine the complete mission architecture with respect to multiple performance objectives. These objectives were defined as the minimisation of the total transfer duration and simultaneously the gross vehicle mass in LEO/LMO. Each analysis was completed using a multi-objective optimal control solver for non-linear constrained problems with multiple phases. This solver included an adaptive mesh refinement strategy with which to identify and refine optimal engine switching structures with respect to each objective.

Of particular interest were the relative durations between the three primary mission segments (outbound, stay, inbound). More specifically, the effect on the allowable stay time at Mars with respect to the minimisation of total time spent in transfer. It was found that mission profiles seemed to conform to distinct groups of solutions within objective space. This suggests a quantifiable set of transfer opportunities/mission profiles differentiated by total propellant requirement and desired duration of surface activities at Mars.

An additional finding was the universal agreement to reduce the size of the propulsion system to the lower end of the performance spectrum represented by the developed NTP sizing relationships. Whilst these performance requirements still represent a fundamental shift from traditional Chemical Propulsion systems (particularly in terms of Specific Impulse), the implication is that current and/or future development of NTP technology would benefit from a focus on improving system reliability rather than base performance statistics. This could include investigations into, for example, extended operational cycles and restartability,

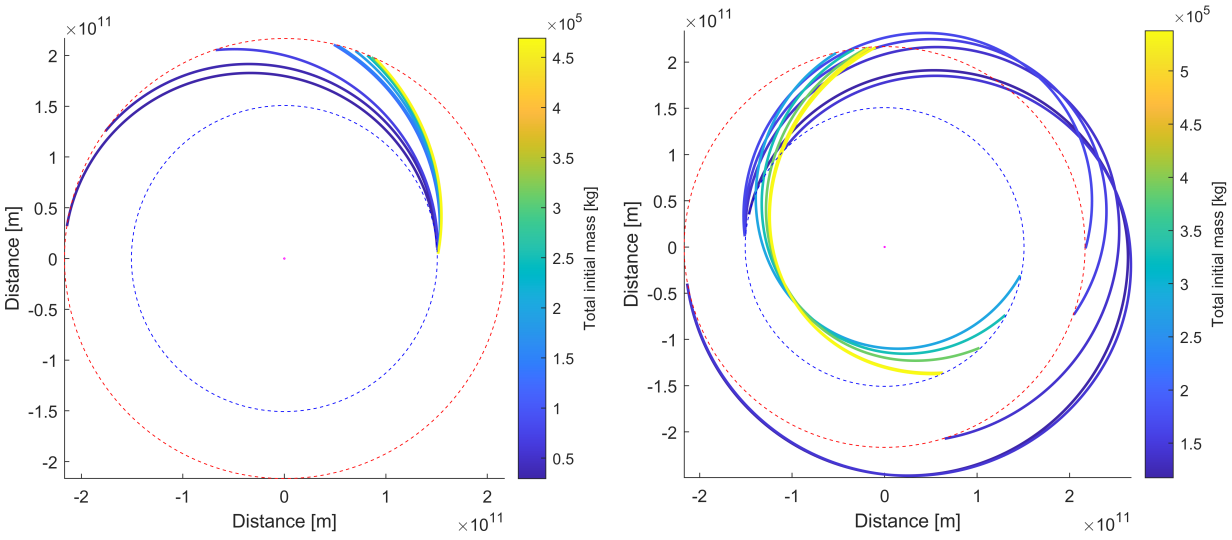

Figure 7: Multi-Objective solutions for (a) the outbound EM transfer and (b) the inbound ME transfer.

Acknowledgements

This work was partially funded through a grant by the European Space Agency General Support Technology Programme (ESA 3-16642/20/NL/MG/rk).

References

[1] C. Bruno and C. Dujarric, "In-space nuclear propulsion," *Acta Astronautica*, vol. 82, no. 2, pp. 159–165, 2013.

[2] L. R. Shepherd and A. V. Cleaver, "The atomic rocket. I," *J. Brit. Interplanetary Soc.*, vol. 7, 1948.

[3] V. Zakirov and V. Pavshook, "Russian Nuclear Rocket Engine Design for Mars Exploration," *Tsinghua Science and Technology*, vol. 12, no. 3, pp. 256–260, 2007.

[4] D. R. Koenig, *Experience Gained from the Space Nuclear Rocket Program (Rover)*. Los Alamos National Laboratory, 1986.

[5] J. Finseth, "Rover nuclear rocket engine program: Overview of rover engine tests, final report," Sverdrup Technology, Tech. Rep., 1991.

[6] W. V. Braun, "Manned Mars Landing: Presentation to the space task group," Tech. Rep., 1969.

[7] E. A. Willis, *Comparison of Trajectory Profiles and Nuclear-propulsion-module Arrangements for Manned Mars and Mars-Venus Missions*. NASA, 1971.

[8] E. National Academies of Sciences, Medicine *et al.*, *Space Nuclear Propulsion for Human Mars Exploration*, 2021.

[9] C. Dujarric, "A new propulsion concept for interplanetary missions," *ESA Bulletin*, vol. 108, pp. 66–71, 2001.

[10] C. Dujarric, A. Santovincenzo, and L. Summerer, "The nuclear thermal electric rocket: A proposed innovative propulsion concept for manned interplanetary missions," *Progress in Propulsion Physics*, pp. 293–312, 2013.

[11] D. F. Landau and J. M. Longuski, "A reassessment of trajectory options for human missions to Mars," in *Collection of Technical Papers - AIAA/AAS Astrodynamics Specialist Conference*, vol. 2, 2004, pp. 836–871.

[12] P. D. Wooster, R. D. Braun, J. Ahn, and Z. R. Putnam, "Mission design options for human Mars missions," *MARS*, 2007.

[13] D. F. Landau and J. M. Longuski, "Trajectories for Human Missions to Mars, Part I: Impulsive Trans-

fers," *Journal of Spacecraft and Rockets*, vol. 43, no. 5, pp. 1035–1042, 2006.

[14] R. M. Zubrin, D. A. Baker, and O. Gwynne, "Mars direct: A simple, robust, and cost effective architecture for the space exploration initiative," *Science and Technology Series*, vol. 89, pp. 275–314, 1991.

[15] H. W. Loeb, V. G. Petukhov, G. A. Popov, and A. I. Mogulkin, "A realistic concept of a manned Mars mission with nuclear-electric propulsion," *Acta Astronautica*, vol. 116, pp. 299–306, 2015.

[16] B. G. Drake, "Human exploration of mars design reference architecture 5.0," NASA, Tech. Rep., 2009.

[17] P. R. Chai, K. T. McBrayer, A. C. McCrea, R. G. Merrill, A. Prasad, and M. Qu, "Crewed mars mission mode options for nuclear electric/chemical hybrid transportation systems," *Accelerating Space Commerce, Exploration, and New Discovery conference, ASCEND 2021*, 2021.

[18] A. C. Owens, C. A. Jones, W. M. Cirillo, J. J. Klovstad, E. L. Judd, P. R. Chai, R. G. Merrill, A. Prasad, J. Cho, and C. Stromgren, "Integrated crewed mars mission analysis, part ii: The trajectory strikes back," *Accelerating Space Commerce, Exploration, and New Discovery conference, ASCEND 2021*, 2021.

[19] S. R. Oleson, L. Burke, L. Dudzinski, J. Fittje, L. S. Mason, T. Packard, P. Schmitz, J. Gyekenyesi, and B. Faller, "A Combined Nuclear Electric and Chemical Propulsion Vehicle Concept for Piloted Mars Opposition Class Missions," no. January 2021, 2020.

[20] M. Durante, "Space radiation protection: destination mars," *Life sciences in space research*, vol. 1, pp. 2–9, 2014.

[21] J. T. Walton, "An overview of tested and analyzed NTP concepts," in *AIAA/NASA/OAI Conference on Advanced SEI Technologies*, 1991.

[22] A. S. Koroteev, V. N. Akimov, N. I. Arkhangel'skii, E. Y. Kuvshinova, and E. I. Muzychenko, "Nuclear Rocket Motors: Development Status and Application Prospects," *Atomic Energy*, vol. 124, no. 4, pp. 244–250, 2018.

[23] N. Frischauf and B. A. Hamilton, "Space nuclear power and propulsion - A basic tool for the manned exploration of the solar system," in *International Congress on Advances in Nuclear Power Plants*, 2004.

[24] C. R. Joyner, M. Eades, J. Horton, T. Jennings, T. Kokan, D. J. H. Levack, B. J. Muzek, and C. B. Reynolds, "LEU NTP Engine System Trades and Mission Options," *Nuclear Technology*, vol. 206, no. 8, pp. 1140–1154, 2020.

[25] C. Maddock, B. Parsonage, L. A. Ricciardi, M. Vasile, and O. Cohen, "Design optimisation and analysis of very high power transportation system to mars," in *72nd International Astronautical Congress*, 2021.

[26] J. M. Salotti, R. Heidmann, and E. Suhir, "Crew size impact on the design, risks and cost of a human mission to Mars," in *IEEE Aerospace Conference Proceedings*, 2014.

[27] M. A. Simon, M. Clowdsley, and S. Walker, "Habitat design considerations for implementing solar particle event radiation protection," *43rd International Conference on Environmental Systems*, 2013.

[28] P. Lopez, E. Schultz, B. Mattfeld, C. Stromgren, and K. Goodliff, "Logistics needs for potential deep space mission scenarios post Asteroid Redirect crewed Mission," in *IEEE Aerospace Conference Proceedings*, 2015.

[29] M. Durante and C. Bruno, "Impact of rocket propulsion technology on the radiation risk in missions to Mars," *European Physical Journal D*, vol. 60, no. 1, pp. 215–218, 2010.

[30] M. Durante and F. A. Cucinotta, "Physical basis of radiation protection in space travel," *Reviews of Modern Physics*, vol. 83, no. 4, 2011.

[31] F. Ferraro, R. D'elia, S. Paternostro, A. Simonetti, and C. Bruno, "Analysis of a manned mars mission with Nuclear Electric Propulsion system," in *60th International Astronautical Congress*, 2009.

[32] R. X. Lenard, "Review of reactor configurations for space nuclear electric propulsion and surface power considerations," in *Nuclear Space Power and Propulsion Systems*, C. Bruno, Ed. AIAA Progress in Astronautics and Aeronautics, 2008.

[33] B. Parsonage and C. Maddock, "A multiresolution method for solving multi-objective optimal control

problems," *Journal of Guidance, Control, and Dynamics*, Accepted August 2024.

[34] Parsonage and Maddock, "Biased dyadic crossover for variable-length multi-objective optimal control problems," in *2024 IEEE Congress on Evolutionary Computation (CEC)*. IEEE, 2024, pp. 1–9.